Published in final edited form as:
Epilepsia. 2008 November ; 49(11): 1925–1940. doi:10.1111/j.1528-1167.2008.01707.x.

FOCAL GENERATION OF PAROXYSMAL FAST RUNS DURING ELECTROGRAPHIC SEIZURES

Sofiane Boucetta[1], **Sylvain Chauvette**[1], **Maxim Bazhenov**[2], and **Igor Timofeev**[1]
[1]Department of Anatomy and Physiology Laval University, Quebec, Canada G1K 7P4
[2]The Salk Institute, Computational Neurobiology Laboratory, La Jolla, CA 92037 USA

Abstract

Purpose—A cortically generated Lennox-Gastaut type seizure is associated with spike-wave/polyspike-wave discharges at 1.0–2.5 Hz and fast runs at 7–16 Hz. Here we studied the patterns of synchronization during runs of paroxysmal fast spikes.

Methods—Electrographic activities were recorded using multisite intracellular and field potential recordings in vivo from cats anesthetized with ketamine-xylazine. In different experiments, the recording electrodes were located either at short distances (<1 mm) or at longer distances (up to 12 mm). The main experimental findings were tested in computational models.

Results—In the majority of cases, the onset and the offset of fast runs occurred almost simultaneously in different recording sites. The amplitude and duration of fast runs could vary by orders of magnitude. Within the fast runs, the patterns of synchronization recorded in different electrodes were as following: (i) synchronous, in phase, (ii) synchronous, with phase shift, (iii) patchy, repeated in phase/phase shift transitions and (iv) non-synchronous, slightly different frequencies in different recording sites or absence of oscillatory activity in one of the recording sites; the synchronous patterns (in phase or with phase shifts) were most common. All these patterns could be recorded in the same pair of electrodes during different seizures and they were reproduced in a computational network model. Intrinsically-bursting (IB) neurons fired more spikes per cycle than any other neurons suggesting their leading role in the fast run generation.

Conclusions—Once started, the fast runs are generated locally with variable correlations between neighboring cortical foci.

Keywords

Synchronization; cortex; electrographic seizures; EEG; intracellular; in vivo; computational model

Introduction

Sleep related epilepsy is characterized by seizures developing during periods of slow-wave sleep. Studies on experimental animals point to the intracortical origin of some specific types of such seizures (Steriade & Contreras 1998). These seizures are characterized by spike-wave (SW) or spike-wave/polyspike-wave (SW/PSW) complexes of 1–2.5 Hz, intermingled with episodes of fast runs at ~7–16 Hz (Neckelmann, et al. 1998, Steriade, et al. 1998a, Steriade & Contreras 1998, Timofeev, et al. 1998). The evolvement of these seizures from the cortically generated slow oscillation may be shaped by the thalamus

Corresponding author: Igor Timofeev, Phone: 418-663-5747 ext. 6396; Fax 418-663-8756; e-mail: Igor.Timofeev@phs.ulaval.ca.
Disclosure of conflicts of interest: None

(Steriade & Contreras 1995, Steriade, et al. 1998a, Steriade & Timofeev 2001, Hughes, et al. 2002, Meeren, et al. 2002). The electrographical pattern of these seizures as well as their occurrence during slow-wave sleep resembles the seizures accompanying Lennox-Gastaut syndrome of humans (Halasz 1991, Kotagal 1995, Niedermeyer 2005a, Niedermeyer 2005b). The prolonged (more than 2–3 s) periods of runs of fast EEG spikes were usually associated with tonic components of seizures accompanying Lennox-Gastaut syndrome (Niedermeyer 2005a). Less frequently fast runs occur in other epileptic conditions (Niedermeyer 2005a). The detailed pattern of synchronization as well as the cellular basis of fast runs is not well understood. Previous single-case human study has shown that an increase in the synchronization stops the runs of fast EEG spikes (Ferri, et al. 2004). Animal studies showed that (a) the thalamus is not involved in the generation of fast runs (Timofeev, et al. 1998), (b) the inhibitory activities in neocortex are impaired during the fast runs (Timofeev, et al. 2002), and (c) these changes occur in parallel with a decrease in the neuronal input resistance (Matsumoto, et al. 1969, Neckelmann, et al. 2000, Timofeev, et al. 2002) and a decrease in the concentration of extracellular calcium (Heinemann, et al. 1977, Amzica, et al. 2002).

During normal (not paroxysmal) brain activities, both the excitatory and inhibitory synaptic interactions provide mechanisms for the synchronization among neighboring recording sites. In a condition of low extracellular Ca^{2+} concentration (decrease in synaptic interactions), impaired inhibitory activities, and low input resistance, as observed during seizures (see above), the synchrony should be reduced. Thus, we hypothesize that paroxysmal runs of fast EEG spikes are generated more locally (compare with normal electrophysiological activities) with minimal, if any, involvement of long-range connections; neighboring foci oscillate in a quasi-independent manner. The present study supports this hypothesis and provides data on the neuronal basis and patterns of synchronization during fast runs generated within spontaneous electrographic seizures. The present study also contains a network model that reproduces the main patterns of synchronization encountered with in vivo recordings and that supports the presented hypothesis.

Materials and methods

In vivo experiments

Experiments were conducted on adult cats anesthetized with ketamine-xylazine anesthesia (10–15 and 2–3 mg/kg i.m., respectively). The animals were paralyzed with gallamine triethiodide (20 mg/kg) after the EEG showed typical signs of deep general anesthesia, essentially consisting of a slow oscillation (0.5–1 Hz). Supplementary doses of the same anesthetics (5 and 1 mg/kg) or simply ketamine (5 mg/kg) were administered at the slightest changes toward the diminished amplitudes of slow waves. The cats were ventilated artificially with the control of end-tidal CO_2 at 3.5–3.7%. The body temperature was maintained at 37–38°C and the heart rate was ~90–100 beats/min. For intracellular recordings, the stability was ensured by the drainage of cisterna magna, hip suspension, bilateral pneumothorax, and by filling the hole made for recordings with a solution of 4% agar. At the end of experiments, the cats were given a lethal dose of pentobarbital (50 mg/kg i.v.). All experimental procedures were performed according to NIH and national guidelines and were approved by the committee for animal care of Laval University.

Single, dual, triple, or quadruple intracellular recordings from suprasylvian associative areas 5 and 7 were performed using glass micropipettes filled with a solution of 3 M potassium-acetate (KAc). A high-impedance amplifier with active bridge circuitry was used to record the membrane potential (V_m) and inject current into the neurons. Field potentials were recorded in the vicinity of impaled neurons and also from more distant sites, using bipolar coaxial electrodes, with the ring (pial surface) and the tip (cortical depth) separated by 0.8–1

mm. In 12 cats, arrays of 7 or 8 low impedance tungsten electrodes, ~1.5 mm apart, were inserted along the suprasylvian gyrus. All electrical signals were sampled at 20 kHz and digitally stored on Vision (Nicolet, Wisconsin, USA). Offline computer analysis of electrographic recordings was done with IgorPro software (Lake Oswego, Oregon, USA). Statistical analysis was conducted with JMP software (Cary, North Carolina, USA). All numerical values are expressed as a mean ± standard deviation.

Computational models

A cortical model consisting in a one-dimensional chain of 100 PY neurons and 25 INs was simulated. The connection fan out was ± 5 neurons for AMPA-mediated PY-PY synapses, ± 1 neuron for AMPA-mediated PY-IN synapses, ± 5 neurons for $GABA_A$-mediated IN-PY synapses. All AMPA- and $GABA_A$-mediated synapses were modeled by first-order activation schemes (Destexhe, et al. 1994), and the expressions for the kinetics are given elsewhere (Bazhenov, et al. 1998). A simple model of synaptic plasticity (USE=7%, τ=700 ms) was used to describe depression of synaptic connections (Abbott, et al. 1997, Tsodyks & Markram 1997, Bazhenov, et al. 1998, Galarreta & Hestrin 1998, Timofeev, et al. 2000). A maximal synaptic conductance was multiplied to depression variable, $D \leq 1$, representing the amount of available "synaptic resources": $D = 1 - (1 - D_i(1-U)) \exp(-(t-t_i)/\tau)$, where U=0.07 is the fraction of resources used per action potential, τ = 700 ms the time constant of recovery of the synaptic resources, D_i the value of D immediately before the i_{th} event, and $(t - t_i)$ the time after i_{th} event.

Each PY and IN cell was modeled by two compartments that included fast Na^+ channels, I_{Na}, and a persistent sodium current, $I_{Na(p)}$, (Alzheimer, et al. 1993, Kay, et al. 1998) in the axo-somatic and the dendritic compartments (Mainen & Sejnowski 1996). A slow voltage-dependent non-inactivating K^+ current, I_{Km}, a slow Ca^{2+} dependent K^+ current, $I_{K(Ca)}$, a high-threshold Ca^{2+} current, I_{Ca}, hyperpolarization-activated depolarizing current, I_h, were included in the dendritic compartment. A fast delayed rectifier potassium K^+ current, I_K, was present in the axo-somatic compartment. The expressions for the voltage- and Ca^{2+}-dependent transition rates for all other currents are given in (Bazhenov, et al. 2002, Frohlich & Bazhenov 2006). Reversal potentials for all K^+-mediated currents were calculated using Nernst equation. The extracellular K^+ concentration was continuously updated based on K^+ currents, K^+ pumps, K^+ buffering simulating the glial K^+ uptake system (Bazhenov, et al. 2004). The glial buffering was modeled by first order kinetics (Kager, et al. 2000). The firing properties of this two compartments model depend on the coupling conductance between compartments (g=1/R, where R is resistance between compartments), and the ratio of dendritic area to axo-somatic area. The ratio, r, controls the firing patterns in the model (Mainen & Sejnowski 1996). We used a model of a regular-spiking neuron for PY cells (r = 165) and a model of a fast-spiking neuron for IN cells (r = 50). The firing patterns of these cell types in response to DC pulses of different amplitude are shown in our previous publication (Fig. 3 B in (Rulkov, et al. 2004)).

Results

In vivo experiments

Experimental model and database—We performed various experiments to study different aspects of thalamocortical physiology between years 2001 and 2006. During these experiments, some of the cats displayed electrographic seizures. In these animals we stopped the initially thought experiment, and changed experimental approach to address the hypothesis described in the introduction of the present study. We recorded electrophysiological activities from 87 cats initially anesthetized with ketamine-xylazine. Typically, supplementary doses of anesthesia were administrated every hour. In 41 cats, an

initial anesthesia was followed by additional doses of ketamine. Similar to other studies (Steriade & Contreras 1995), in these experiments ~30 % of cats (12 cats out of 41) developed spontaneous paroxysmal discharges. Adding ketamine-xylazine as supplementary anesthetic resulted in the generation of electrographic seizures in ~75% of cats (35 out of 46). Usually, the seizures started after administration of the third-fourth supplementary dose. These seizures, consisting of SW complexes at 1–2.5 Hz or SW/PSW complexes associated with fast runs at 7–16 Hz, were developed from sleep-like slow rhythm. As in our previous study (Grenier, et al. 2003b), the seizures were preceded by ripples or the onset of seizures occurred simultaneously with them in at least one recording electrode (not shown). In total, we analyzed 224 electrographic seizures recorded with field potential electrodes. In parallel with EEG recording, we recorded intracellular activities of 157 neurons. This includes 8 simultaneous quadruple, 15 triple, and 22 dual records. In 11 neurons, we recorded more than 20 seizures.

An example of typical seizure is shown in Fig. 1 A in which the first 5 s show a normal slow oscillation. The beginning of electrographic seizure was associated with ampler EEG waves and ampler intracellularly recorded depolarizing potentials repeated at frequencies 1.0–2.5 Hz. Examples of transition from slow oscillation to seizures at larger scale could be found in our previous publications (Figs 1–2 in (Timofeev, et al. 1998), Fig. 10 (Timofeev, et al. 2002), Fig. 8 (Frohlich, et al. 2006)). In some neurons, the enhanced depolarizing potentials were associated with an increased firing (as in neuron 1 and neuron 4 in Fig. 1). After several cycles of SW/PSW discharges the activity switched to runs of paroxysmal spikes (7–16 Hz) during which the long-lasting depth-positive EEG waves and associated intracellular hyperpolarizing potentials were absent. The fast runs appeared as a prolongation of PSW complexes. In this study, the polyspike discharges exceeding 1 s were considered as runs of fast EEG spikes. The total duration of seizures was between 10 and 120 s (37.2±2.2 s, mean ±SD, Fig. 1 C). We analyzed 252 periods of fast runs, which lasted between 1 and 30 s (4.9±5.7 s, Fig. 1 C). Out of these, 174 periods lasted for less than 5 seconds. Each electrographic seizure recorded in these experimental conditions could have several periods of fast runs (1–8, mean 2.4±1.4, Fig. 1, C), and SW complexes. Below, we will focus on the generation of paroxysmal runs of fast spikes.

Multisite distant recordings during fast runs—Using multisite recordings, we evaluated the patterns of synchronization between field potentials and intracellular activities during fast runs. Within the fast runs, the patterns of synchronization recorded with different electrodes were as following: (a) synchronous, in phase, (b) synchronous, with phase shift (one recording preceded or followed the activity in reference electrode), (c) “patchy” repeated in phase/phase shift transitions, and (d) non-synchronous, different frequencies in different recording sites or absence of rhythmic activities at one of the recording sites (see Fig. 4C). All these patterns could be recorded in the same pair of electrodes during different seizures. Generally, the frequency of activity during the same period of relatively short (<5 s) fast runs remained similar in different recording sites, but the phase-shifts were very variable during different epochs of the fast runs. Some of these patterns are illustrated in Fig. 1 where a field potential recording and a quadruple intracellular recording were used. In this experiment, the electrodes were located in the suprasylvian gyrus: intra-cell 1 was located in the anterior part of area 5, the other electrodes were equally spaced with a distance between neighboring electrodes of about 4 mm in the posterior direction. The seizure contained three periods of fast runs (two of them are shown at a higher time resolution in the Fig. 1A, b). During the *first* period of fast runs the maximal depolarization of neurons 1, 2, and 3 preceded the maximal field potential depth-negativity and the maximal depolarization of neuron 4 followed the field potential (see black lines in Fig. 1 A and B). The onset of each oscillatory cycle occurred first at the electrode Intra-cell 2 (see blue dotted lines in Fig. 1) during all the cycles of this period of fast runs (Fig. 1 B). During the *second* period of fast

runs, Intra-cell 1 was always the first in the generation of each oscillatory cycle. The onset of depolarization in neuron 2, occurred coincidentally with the spike in the neuron 1; the onset of depolarization in the neuron 3 was delayed, and the delay fluctuated in 20–30 ms range. The oscillatory activity in the neuron 4 was damped and the neuron 4 revealed a patchy pattern of activity: there was a phase shift during each several cycles (Fig. 1, B). Thus, the multisite intracellular and field potential recordings revealed that runs of fast spikes behave as quasi-independent oscillators (see also (Derchansky, et al. 2006)).

To characterize the patterns of synchronization during fast runs, we performed cross-correlation analysis. As expected, during the SW/PSW complexes, the cross-correlation between intracellular activities and EEG was generally negative since active periods were characterized by neuronal depolarization and depth-negative EEG waves, and during depth-positive EEG waves the neurons were hyperpolarized (Fig. 2). The fast runs were characterized by variable patterns of synchronization. In the majority of cases (70 %), the delay between the two recording leads was stable throughout the period of fast runs. As shown in the example in Fig. 2 B, the Intra-cell 1 preceded the EEG by about 35 ms during the first period of fast runs. However, during the second period of fast runs, the intracellular activities of this neuron preceded the EEG during the first half and it was synchronous in phase oscillation during the second half of the same period of fast runs. The second neuron (Intra-cell 2) and EEG had stable relation during fast runs and the maximum of neuronal excitation preceded the EEG with delay of about 10 ms during both periods of fast runs (Fig. 2 B). Therefore the neuron 1 revealed patchy pattern suggesting that fast runs are generated with very limited, in any, communication between cortical foci.

Although in the vast majority of cases the periods of fast runs occurred almost simultaneously in all recording leads along the suprasylvian gyrus, on some occasions, the pattern was different. The Fig. 3 shows an example in which the seizure started from the fast run generated in the anterior part of suprasylvian cortex (EEG 7). The correlation between anterior and posterior electrodes had small values (Fig. 3 B, 1). Progressively, this activity involved more posterior regions of suprasylvian gyrus and the oscillation with a frequency of 11 Hz becomes dominant on all 7 EEG leads with a high value of correlation accompanied by a rapid propagation of activity in posterior-anterior direction (Fig. 3 B, 2). Another period of the fast runs, during the same seizure, started almost simultaneously in all EEG electrodes (frequency 8.5 Hz, see the middle expanded part in Fig. 3 A), and the correlation between all electrodes was high with a marked anterior-posterior propagation (Fig. 3 B, 3). At the end of the seizure, the fast runs (9.5 Hz) were dominant in the posterior part of suprasylvian gyrus, while the anterior suprasylvian gyrus displayed frequency around 4 Hz, therefore the anterior-posterior correlation was low (Fig. 3 B, 4).

Thus, our multisite recordings (both intra- and extracellular) demonstrated that in the majority of cases the onset and the end of runs of fast spikes occurred almost simultaneously at different locations. However, either the frequency of oscillation or the phase shifts between different locations were dissimilar in each period of fast runs. The dominating pattern of activity could switch even during the same epoch of fast runs.

Divergence of synchronizing patterns during fast runs—The phase shift during the same run of fast spikes could be very variable when it is recorded with two or more electrodes located at distances larger than several millimeters (Fig. 1–Fig. 3). In long-lasting recordings (longer than 10 min), we analyzed the patterns of synchronization during fast runs between neurons and field potential recorded at about 1 mm apart (Fig. 4). We found that each pair of records (cell-EEG) had a preferred phase relationship, but on some occasions, it revealed significant variations in the pattern of synchronization. Even in close recordings the pattern of synchronization during fast runs could vary within the same

seizure. During one period of fast runs, the oscillation in two electrodes could be synchronous, while during another period it could be of different frequencies (Fig. 4). As an extreme case, we recorded large amplitude EEG fast runs and absence of such or similar oscillation in a closely located neuron (n=5), while the previous or the following periods of fast runs showed synchronous oscillations in both electrodes (not shown). We analyzed the pattern of synchronization between activities recorded with intracellular and nearby field potential electrodes during 312 periods of fast runs (Fig. 4, C). We found that in only 20 % of cases the oscillation was in phase (the neuron fired around maximum of the EEG depth-negative wave). However, the phase-locked patterns of activity (with or without different delays) were recorded in 70% of cases. In 22 % of cases the activity was not synchronous: either two sites revealed oscillation with different frequencies or the recording revealed arrhythmic activity (Fig. 4, C). In 8% of cases the activity was patchy; there were two or more changes in the pattern of synchronization during the same period of fast run (see examples in Fig. 1, intra-cell 4, second period and Fig. 2 Intra-cell 1, second period).

We systematically analyzed the spatial synchronization of fast runs within suprasylvian gyrus of cats. For this analysis, we have chosen only periods of fast runs that revealed consistent delays of coherent activity over 10 or more consecutive cycles with variability of crosscorrelation maximums not exceeding 2 ms (Fig. 5). We analyzed separately pairs of EEG recordings and pairs of intracellular recordings obtained at different distances. In most of the cases, the activity in the more anterior electrodes preceded the activity in the more posterior electrodes. We found that the fast run activity could propagate with a maximal velocity reaching 10 m/s; however, the mean velocity was estimated as 2.13±0.38 m/s from pairs of EEG electrodes and 2.23±0.60 m/s from pairs of cells, indicating the presence of similar delays detected with two different methods of recordings. During consecutive fast runs, the same pair of either EEG or intracellular recordings could reveal propagation from −5 m/s (posterior to anterior) to 8 m/s (anterior to posterior). Thus, each period of fast runs was characterized by unique propagation velocity and direction of propagation. However, the recordings from closely located neurons (<0.2 mm lateral distance) revealed that the coherent oscillation between two neurons could be delayed by up to 20 ms, which corresponds to very slow propagation speed of <10 mm/s. This suggests that these two cells were oscillating in an independent manner. Thus, similar to studies in desinhibited slices, if propagation of activity takes place, its velocity varied manifold (Chervin, et al. 1988).

In a sample of 115 periods of fast runs that lasted 5 s or longer we analyzed the duration of oscillatory cycles (Fig. 6). The frequency of oscillation during the prolonged periods (>10 s) of fast runs usually underwent a progressive decrease (Fig. 6, B). To estimate the duration of a cycle during different periods of the same fast run, we obtained autocorrelations for consecutive periods lasting 5 s (Fig. 6 C). At the beginning of the prolonged fast runs the mean frequency of oscillation was 13.8±2.0 Hz and at the end, it was slightly but significantly slower 11.3±2.1 Hz (paired t-test, p=0.007). The decrease in frequency on cycle-by-cycle basis was 0.036±0.016 Hz. The duration of cycles for neurons and EEG was usually similar and varied from 62 ms to 124 ms (16 Hz to 8 Hz, Fig. 6, D 1, E 1). However, during some period of fast runs the difference could be as large as a double of the frequency. We calculated rhythm coefficient, measured as the amplitude of the second peak of autocorrelation, being 1 when all cycles had identical frequency and 0 when all cycles had different frequency. The rhythm coefficient obtained from the field potential recordings during fast runs was very high, and for 75% of cases it was above 0.8, suggesting a high periodicity of cycles (Fig. 6 E 2). The intracellular traces revealed slightly lower values of correlation (Fig. 6 D 2, E 2). This was likely because the variability of cycle duration for one neuron was larger than for field potential recordings; field potentials reflect the averaged activity of a set of neurons and glial cells and thus, they are much less sensitive to the variability in individual cycles of individual cells.

Membrane potential during fast runs—The membrane potential during SW components of seizures had a bimodal distribution and exposed two relatively stable states. In the recording shown in (Fig. 7, A) the neuron was hyperpolarized to −80 mV during EEG wave component and it was depolarized to −55 mV during EEG spike component as revealed by the histogram of membrane potential distribution (Fig. 7, B). During fast runs, the membrane potential oscillated continuously and only one peak could be detected from the histogram of membrane potential distribution which was in between the peak values of membrane potential during de- and hyperpolarized states (Fig. 7, B). To quantify the peak values of membrane potential in a population of neurons we used the modal values for de- and hyperpolarized states and fast runs. The histograms of membrane potential distribution for 50 neurons demonstrate that the majority of neurons had their modal membrane potential values during fast runs between that of de- and hyperpolarized states during SW complexes (Fig. 7, C). The membrane potential during fast runs was by 9.11±1.13 mV ($p<0.0001$) more hyperpolarized than during the depolarized components of SW discharges. There were significant correlations ($r=0.57$, $p<0.0001$) between the membrane potential during fast runs and depolarizing component of seizures.

Intrinsic neuronal properties and fast runs—All neurons that were recorded during both, electrographic seizures and periods outside seizures (n=157), were classified by electrophysiological criteria as regular-spiking (RS), fast-rhythmic-bursting (FRB), intrinsically-bursting (IB), and fast-spiking (FS) (Connors & Gutnick 1990, Gray & McCormick 1996, Steriade, et al. 1998b). The electrophysiological classification of neurons was performed during periods of normal (not paroxysmal) activity. In this set of experiments, we identified 70.6 % of neurons as RS, 11.8 % as FRB, 11.8 % as IB, and the remaining 6 neurons were FS. In each of these neurons, we calculated the mean number of spikes per cycle generated during fast runs (Fig. 8). At least 100 cycles were counted to obtain a mean number of spikes generated by one neuron. Since in many instances the amplitude of spikes was significantly reduced as compared to spikes occurring outside seizures, we counted only spikes that were at least a half of amplitude of a mean spike recorded during normal activities. Some neurons revealed a large variability in the number of spikes per cycle, which could fluctuate from 1 to 6 (Fig. 1, Intra – cell 1). Statistically, we found however that the number of spikes per cycle generated by IB and FRB neurons was significantly higher (Tukey-Kramer HSD test) than the number of spikes generated by other types of neurons (Fig. 8). In addition, IB cells were usually depolarized and fired before any other type of neurons (Fig. 8, bottom panel).

Since, in all the recorded combinations, we observed either repeatable phase shifts or absence of synchrony; our data suggest that fast paroxysmal runs are generated locally. We used a highly simplified network model to demonstrate how extremely variable phase relations can indeed develop between synaptically coupled, oscillating neurons.

Computational model—We have previously shown in a model of isolated cortical pyramidal (PY) neuron that increases in $[K^+]_o$ could lead to slow 2–3 Hz oscillations and fast runs (Bazhenov, et al. 2004). Here we explore phase relations between neurons in different oscillatory states and we show effect of synaptic interaction on network synchronization.

To study synchrony of population oscillations during different oscillatory regimes, we simulated a network model of 100 PY neurons and 25 interneurons (INs). An external stimulus (DC pulse of 10s) was applied to the network to induce high frequency spiking in PY cells. Upon DC stimulus termination, all the neurons displayed slow bursting (*SW*) followed by fast spiking (*fast runs*) (Fig. 9A). We found that: (1) bursting mechanism in this model is essentially mediated by the dynamic interaction of the high threshold calcium and

the calcium-activated potassium conductances in PY neurons; (2) progressive decrease of $[K^+]_o$ leads to transition between slow bursting and fast runs; (3) low activity of inhibitory interneurons during fast runs can explain reduced synchrony of these oscillations compare with slow bursting activity.

Because of random variability of the model parameters across neurons and different initial conditions, the neurons in the network model fired independently when synaptic coupling was turned off (Fig. 9 A, top). Slow bursting lasted less than 4 seconds. When excitatory/inhibitory coupling between neurons was included, the slow paroxysmal bursting lasted much longer (~10 s) and became synchronized across neurons (Fig. 9 A, bottom). Fig. 9 B shows cross-correlation between neighbor PY cells in the network; during slow paroxysmal oscillations these neurons fired with minimal phase delays. A progressive change of $[K^+]_o$ triggered transition from slow to fast oscillations. Similar to in vivo data, neighbor neurons displayed this transition nearly simultaneously; however we found a few large clusters with very different transition times (compare neurons #1–50 and #51–100 in Fig. 9 A, bottom). Including long-range connections between PY neurons would likely increase the global synchrony of transitions between epochs of slow and fast oscillations. To test this hypothesis we included random long-range connections between PY neurons and varied probability of long-range coupling *P*. When $P > 0.02–0.03$, transition from slow bursting to fast runs occurred almost simultaneously with less than 200 ms variability across all neurons in the network (not shown). Thus, synaptic coupling was sufficient to explain synchrony of slow bursting oscillations and fast-slow-fast transitions. Including long-range connections with such low probability did not produce, however, any systematic effect on phase relations between neurons during fast oscillations (see below).

In contrast to the slow bursting mode, during fast runs the degree of synchrony between neurons (even in close proximity) was significantly reduced even after synaptic coupling was introduced. Typically, neighbor neurons fired with a phase shift, which was consistent for a few cycles of network oscillations thus suggesting local spike propagation. Different cell pairs displayed phase delays of different signs (propagation in different directions). Phase relations between neurons could change from in-phase to out-phase oscillations or vice versa either gradually (see, e.g., cross-correlation plot for PY35 and PY36 in Fig. 9 B) or suddenly (see, e.g., cross-correlation plot for PY35 and PY38 in Fig. 9 B).

These modeling results suggest that synaptic coupling between PY neurons and feedback inhibition from active INs may explain synchrony of slow bursting oscillations. Indeed, after synaptic connectivity was introduced in the model, asynchronous firing in all network states (Fig. 9A top) was replaced by synchronized oscillations in the bursting mode (Fig. 9A, bottom). During fast runs, however, local synaptic excitation, while influenced the phase relations between neighbor neurons, was not sufficient to arrange steady network synchronization. More importantly, the synchronization effect of feedback inhibition was absent during fast runs because of low Ins' spiking activity (Fig. 9C). Random long-range connections increased synchrony of transitions between slow bursting and fast runs but could not enhance synchrony of fast oscillations on cycle-tocycle basis.

Discussion

In this study, we analyzed the spatio-temporal properties of runs of fast EEG spikes recorded during spontaneous seizures in cats anesthetized with ketamine-xylazine and in computational models. We found that (a) the runs of fast EEG spikes with a frequency of 7–16 Hz often accompanied neocortical seizures; (b) the patterns of synchrony during fast runs were: (i) synchronous, in phase, (ii) synchronous, with phase shift, (iii) patchy, repeated in phase/phase shift transitions, and (iv) non-synchronous, different frequencies in different

recording sites or absence of oscillatory activity in one of the recording sites; the synchronous patterns were most common; (c) the runs of fast spikes appeared as quasi-independent oscillators even in neighboring cortical locations suggesting their focal origin; (d) synchronous fast runs propagated in anterior-posterior direction with a velocity of 2.1–2.2 m/s; (e) the membrane potential during fast runs was by ~9 mV less depolarized as compared to the depolarizing components of SW complexes.

Experimental model of paroxysmal activity

Most of the cats anesthetized with ketamine-xylazine anesthesia, followed by supplementary doses of ketamine-xylazine developed paroxysmal activities consisting of SW discharges at 1–2.5 Hz and runs of fast spikes at 7–16 Hz. These seizures are generated neocortically as (a) they could be obtained in athalamic cats (Steriade & Contreras 1998), (b) in small neocortical slabs (Timofeev, et al. 2000) or (c) in the undercut cortex (Topolnik, et al. 2003, Nita, et al. 2006, Nita, et al. 2007) and (d) most of thalamocortical neurons do not fire during this type of seizures (Steriade & Contreras 1995, Pinault, et al. 1998, Timofeev, et al. 1998). The cause of these seizures is unclear. A combination of two major factors could account for the development of those paroxysmal activities.

(a) Slow oscillations—Spontaneously occurring SW complexes at 1–2.5 Hz and fast runs at 7–16 Hz developed without discontinuity from the slow (mainly 0.5–0.9 Hz) cortically generated oscillation (Steriade & Contreras 1995, Steriade, et al. 1998a). Periods of disfacilitation accompanying sleep oscillations activate a large number of intrinsic and synaptic factors leading to the development of seizures (see (Timofeev & Steriade 2004) for the detailed discussion). However, the occurrence of seizures during sleep is far lower than the occurrence of seizures in cats anesthetized with ketamine-xylazine (Steriade, et al. 1998a).

(b) Effects of ketamine-xylazine—Ketamine at anesthetic doses blocks NMDA dependent synaptic events (MacDonald, et al. 1991). An activation of NMDA receptors contributes, but is not essential in the generation of paroxysmal discharges (Barkai, et al. 1994, Traub, et al. 1996). Thus, ketamine should decrease the propensity to the seizure generation. Additional blockage of nicotinic cholinoreceptors by ketamine (Rudolph & Antkowiak 2004) would remove their depolarizing action on thalamocortical neurons (McCormick 1992), low-threshold spiking cortical interneurons (Xiang, et al. 1998), and should reduce the efficacy of excitatory synapses formed by thalamocortical neurons on cortical neurons (Gil, et al. 1997). However, NMDA blockers at low concentrations could elicit epileptiform burst discharges (Gorji & Speckmann 2001, Midzyanovskaya, et al. 2004).

Xylazine is the agonist of alpha-2 adrenoreceptors, heavily present in the neocortex (Hedler, et al. 1981, Nicholas, et al. 1993) that at low doses favors seizures (Joy, et al. 1983) and promotes oscillatory behavior of thalamocortical system (Buzsaki, et al. 1991). Clonidine, a potent agonist of alpha-2 receptors inhibited action potential generation of thalamocortical neurons (Funke, et al. 1993) and induced changes in the spectral content of the EEG (Sitnikova & van Luijtelaar 2005). Finally, norepinephrine application, depolarized thalamocortical neurons, suppressed their bursts, leading to tonic firing (McCormick & Prince 1988). Thus, we suggest that xylazine actions in neocortex largely contribute to the generation of paroxysmal activity induced by ketamine-xylazine anesthesia.

Synaptic interactions and synchronization during seizures

The amplitude of field potentials during SW components of electrographic seizures is higher than the amplitude of slow oscillation (Fig. 2 and Fig. 4). This suggests that the focal

synchronization during seizures is higher than during the normal brain activities. However, the long-range synchronization during seizures is reduced (Neckelmann, et al. 1998,Derchansky, et al. 2006). Our modeling data demonstrate that transient seizure-like activity could be obtained in a single cortical neuron (not shown), if some extracellular conditions (primarily increased $[K^+]_o$) are present. Therefore, the ligand dependent synaptic interactions alone do not explain the generation of some form of paroxysmal activities (Johnston & Brown 1981,Polack & Charpier 2006). Multiple data support this point of view. (a) Paroxysmal activities are associated with a decreased $[Ca^{2+}]_o$ (Heinemann, et al. 1977,Pumain, et al. 1983,Amzica, et al. 2002), and as a consequence, the effectiveness of synaptic strength decreases, but the intrinsic neuronal excitability increases (Hille 2001). (b) The use of low or even 0 mM $[Ca^{2+}]_o$ in hippocampal (Leschinger, et al. 1993,Pan & Stringer 1997,Bikson, et al. 1999) and cortical (Seigneur J., Timofeev I., unpublished data) slices in vitro results in the development of epileptiform discharges. (c) The synaptic responsiveness during electrographic seizures in vivo decreases (Steriade & Amzica 1999,Cisse, et al. 2004) and remain reduced after the end of seizures (Nita, et al. 2008), (d) the long-range synchronization during seizures, particularly during fast runs, is low or absent (Fig. 4), and finally (e) the neuronal firing dramatically reduces toward the end of the seizure, while intracellular and field potential activities are ampler as compared to the beginning of the seizure (Bazhenov, et al. 2004,Timofeev & Steriade 2004). In a condition of reduced efficiency of chemical synaptic transmission, the focal neuronal synchronization could be achieved either via electrical coupling between different groups of neurons (Galarreta & Hestrin 1999,Gibson, et al. 1999,Perez Velazquez & Carlen 2000,Schmitz, et al. 2001), glial cells (Amzica, et al. 2002), or via ephaptic interactions (Taylor & Dudek 1982,Taylor & Dudek 1984a,Taylor & Dudek 1984b,Grenier, et al. 2003a). The mechanisms of electrical coupling have a high efficacy for the short-range synchronization (Galarreta & Hestrin 2001). During fast runs, the activity of FS interneurons is significantly reduced (Timofeev, et al. 2002), and consequently the efficiency of synchronization via electrically coupled interneuronal network (Galarreta & Hestrin 1999,Gibson, et al. 1999,Perez Velazquez & Carlen 2000) is diminished. The amplitude of field potentials is also reduced (Fig. 1–Fig. 5) indicating a reduced neuronal synchrony. All five factors discussed above (a–e) are likely contributing to the remarkable loss of synchrony during fast runs.

The onset and the end of fast run occurred almost simultaneously at large cortical distances (Fig. 1, Fig. 2). In Lennox-Gastaut syndrome patients, the runs of fast EEG spikes arise locally (Ohtahara, et al. 1995), primarily from frontal lobe (Niedermeyer 2005a). In cats, the fast runs are also recorded from precruciate gyrus (see Figs. 2, 4–11 in (Timofeev, et al. 1998)). We demonstrated that fast runs propagate in anterior-posterior direction within suprasylvian gyrus (Fig. 5), likely evolving from frontal cortical areas. The computational model suggests that long-range excitatory connections may account for this synchrony. Another possibility includes the existence of some unknown synchronizing input arriving to the different cortical loci and droving both, the onset, and the end, of fast runs.

Transitions between SW and fast run was also simulated in a cortical column model after fast inhibition was partially blocked (Traub, et al. 2005). To simulate SW like patterns, cortical neurons had to be depolarized, reflecting the depolarizing effects of the elevated extracellular K^+.

Our finding that both IB and FRB neurons fired more spikes during fast runs than the other types of neurons (Fig. 8), imply that bursting neurons could generate the fast runs. The intrinsic tuning of intraburst frequency for FRB neurons is in the range from 20 Hz to 60 Hz (Gray & McCormick 1996,Steriade, et al. 1998b), thus their frequency is much higher than the frequency of paroxysmal fast runs (Fig. 8), and their leading role in the generation of fast runs is doubtful. The intraburst frequency of IB neurons in vivo during normal network

activities is around 8 Hz (Nuñez, et al. 1993) (see also Fig. 8), which is close to the frequency of fast runs. Seizure related changes in extracellular Ca^{2+} and K^{+} concentration (Somjen 2002) could slightly modulate the intraburst frequency of IB neurons and thus to cover all range of fast run frequencies. Thus, we suggest that cortical IB neurons play a role of pacemakers during paroxysmal fast runs.

We conclude that the runs of fast EEG spikes, during cortically generated seizures, are generated as quasi-independent oscillators, with very little synaptic communication within cortical network.

Acknowledgments

We would like to thank P. Giguère for excellent technical assistance. This research was supported by grants from Canadian Institutes of Health Research, Natural Science and Engineering Research Council (I.T.) and NIH-NIDCD (M.B.). I.T. is scholar of Canadian Institutes of Health Research. S.C. is a CIHR fellow. We confirm that we have read the Journal's position on issues involved in ethical publication and affirm that this report is consistent with those guidelines.

References

Abbott LF, Varela JA, Sen K, Nelson SB. Synaptic depression and cortical gain control. Science. 1997; 275:220–224. [PubMed: 8985017]

Alzheimer C, Schwindt PC, Crill WE. Modal gating of Na+ channels as a mechanism of persistent Na + current in pyramidal neurons from rat and cat sensorimotor cortex. J Neurosci. 1993; 13:660–673. [PubMed: 8381170]

Amzica F, Massimini M, Manfridi A. Spatial buffering during slow and paroxysmal sleep oscillations in cortical networks of glial cells in vivo. J Neurosci. 2002; 22:1042–1053. [PubMed: 11826133]

Barkai E, Grossman Y, Gutnick MJ. Long-term changes in neocortical activity after chemical kindling with systemic pentylenetetrazole: an in vitro study. J Neurophysiol. 1994; 72:72–83. [PubMed: 7965034]

Bazhenov M, Timofeev I, Steriade M, Sejnowski TJ. Computational models of thalamocortical augmenting responses. J Neurosci. 1998; 18:6444–6465. [PubMed: 9698334]

Bazhenov M, Timofeev I, Steriade M, Sejnowski TJ. Model of thalamocortical slow-wave sleep oscillations and transitions to activated states. J Neurosci. 2002; 22:8691–8704. [PubMed: 12351744]

Bazhenov M, Timofeev I, Steriade M, Sejnowski TJ. Potassium model for slow (2–3 Hz) in vivo neocortical paroxysmal oscillations. J Neurophysiol. 2004; 92:1116–1132. [PubMed: 15056684]

Bikson M, Ghai RS, Baraban SC, Durand DM. Modulation of burst frequency, duration, and amplitude in the zero-Ca(2+) model of epileptiform activity. J Neurophysiol. 1999; 82:2262–2270. [PubMed: 10561404]

Buzsaki G, Kennedy B, Solt VB, Ziegler M. Noradrenergic Control of Thalamic Oscillation: the Role of alpha-2 Receptors. Eur J Neurosci. 1991; 3:222–229. [PubMed: 12106199]

Chervin RD, Pierce PA, Connors BW. Periodicity and directionality in the propagation of epileptiform discharges across neocortex. J Neurophysiol. 1988; 60:1695–1713. [PubMed: 3143812]

Cisse Y, Crochet S, Timofeev I, Steriade M. Synaptic responsiveness of neocortical neurons to callosal volleys during paroxysmal depolarizing shifts. Neuroscience. 2004; 124:231–239. [PubMed: 14960354]

Connors BW, Gutnick MJ. Intrinsic firing patterns of divers neocortical neurons. Trends Neurosci. 1990; 13:99–104. [PubMed: 1691879]

Derchansky M, Rokni D, Rick JT, Wennberg R, Bardakjian BL, Zhang L, Yarom Y, Carlen PL. Bidirectional multisite seizure propagation in the intact isolated hippocampus: the multifocality of the seizure "focus". Neurobiol Dis. 2006; 23:312–328. [PubMed: 16815026]

Destexhe A, Mainen ZF, Sejnowski TJ. Synthesis of models for excitable membranes, synaptic transmission and neuromodulation using a common kinetic formalism. J Comput Neurosci. 1994; 1:195–230. [PubMed: 8792231]

Ferri R, Stam CJ, Lanuzza B, Cosentino FI, Elia M, Musumeci SA, Pennisi G. Different EEG frequency band synchronization during nocturnal frontal lobe seizures. Clin Neurophysiol. 2004; 115:1202–1211. [PubMed: 15066546]

Frohlich F, Bazhenov M. Coexistence of tonic firing and bursting in cortical neurons. Phys Rev E Stat Nonlin Soft Matter Phys. 2006; 74:031922. [PubMed: 17025682]

Frohlich F, Bazhenov M, Timofeev I, Steriade M, Sejnowski TJ. Slow state transitions of sustained neural oscillations by activity-dependent modulation of intrinsic excitability. J Neurosci. 2006; 26:6153–6162. [PubMed: 16763023]

Funke K, Pape HC, Eysel UT. Noradrenergic modulation of retinogeniculate transmission in the cat. J Physiol. 1993; 463:169–191. [PubMed: 8246181]

Galarreta M, Hestrin S. Frequency-dependent synaptic depression and the balance of excitation and inhibition in the neocortex. Nat Neurosci. 1998; 1:587–594. [PubMed: 10196566]

Galarreta M, Hestrin S. A network of fast-spiking cells in the neocortex connected by electrical synapses. Nature. 1999; 402:72–75. [PubMed: 10573418]

Galarreta M, Hestrin S. Electrical synapses between GABA-releasing interneurons. Nat Rev Neurosci. 2001; 2:425–433. [PubMed: 11389476]

Gibson JR, Beierlein M, Connors BW. Two networks of electrically coupled inhibitory neurons in neocortex. Nature. 1999; 402:75–79. [PubMed: 10573419]

Gil Z, Connors BW, Amitai Y. Differential regulation of neocortical synapses by neuromodulators and activity. Neuron. 1997; 19:679–686. [PubMed: 9331357]

Gorji A, Speckmann EJ. Low concentration of DL-2-amino-5-phosphonovalerate induces epileptiform activity in guinea pig hippocampal slices. Epilepsia. 2001; 42:1228–1230. [PubMed: 11737156]

Gray CM, McCormick DA. Chattering cells: superficial pyramidal neurons contributing to the generation of synchronous oscillations in the visual cortex. Science. 1996; 274:109–113. [PubMed: 8810245]

Grenier F, Timofeev I, Crochet S, Steriade M. Spontaneous field potentials influence the activity of neocortical neurons during paroxysmal activities in vivo. Neuroscience. 2003a; 119:277–291. [PubMed: 12763088]

Grenier F, Timofeev I, Steriade M. Neocortical very fast oscillations (ripples, 80–200 Hz) during seizures: intracellular correlates. J Neurophysiol. 2003b; 89:841–852. [PubMed: 12574462]

Halasz P. Runs of rapid spikes in sleep: a characteristic EEG expression of generalized malignant epileptic encephalopathies. A conceptual review with new pharmacological data. Epilepsy Res Suppl. 1991; 2:49–71. [PubMed: 1662048]

Hedler L, Stamm G, Weitzell R, Starke K. Functional characterization of central alpha-adrenoceptors by yohimbine diastereomers. Eur J Pharmacol. 1981; 70:43–52. [PubMed: 6260514]

Heinemann U, Lux HD, Gutnick MJ. Extracellular free calcium and potassium during paroxsmal activity in the cerebral cortex of the cat. Exp Brain Res. 1977; 27:237–243. [PubMed: 880984]

Hille, B. Ionic channels of excitable membranes. Sunderland, Massachusetts: Sinauer Associates INC; 2001.

Hughes SW, Cope DW, Blethyn KL, Crunelli V. Cellular mechanisms of the slow (<1 Hz) oscillation in thalamocortical neurons in vitro. Neuron. 2002; 33:947–958. [PubMed: 11906700]

Johnston D, Brown TH. Giant synaptic potential hypothesis for epileptiform activity. Science. 1981; 211:294–297. [PubMed: 7444469]

Joy RM, Stark LG, Albertson TE. Dose-dependent proconvulsant and anticonvulsant actions of the alpha 2 adrenergic agonist, xylazine, on kindled seizures in the rat. Pharmacol Biochem Behav. 1983; 19:345–350. [PubMed: 6314391]

Kager H, Wadman WJ, Somjen GG. Simulated seizures and spreading depression in a neuron model incorporating interstitial space and ion concentrations. J Neurophysiol. 2000; 84:495–512. [PubMed: 10899222]

Kay AR, Sugimori M, Llinas R. Kinetic and stochastic properties of a persistent sodium current in mature guinea pig cerebellar Purkinje cells. J Neurophysiol. 1998; 80:1167–1179. [PubMed: 9744930]

Kotagal P. Multifocal independent Spike syndrome: relationship to hypsarrhythmia and the slow spike-wave (Lennox-Gastaut) syndrome. Clin Electroencephalogr. 1995; 26:23–29. [PubMed: 7882540]

Leschinger A, Stabel J, Igelmund P, Heinemann U. Pharmacological and electrographic properties of epileptiform activity induced by elevated K+ and lowered Ca2+ and Mg2+ concentration in rat hippocampal slices. Exp Brain Res. 1993; 96:230–240. [PubMed: 7903641]

MacDonald J, Bartlett M, Mody I, Pahapill P, Reynolds J, Salter M, Schneiderman J, Pennefather P. Actions of ketamine, phencyclidine and MK-801 on NMDA receptor currents in cultured mouse hippocampal neurones. J Physiol (Lond). 1991; 432:483–508. [PubMed: 1832184]

Mainen ZF, Sejnowski TJ. Influence of dendritic structure on firing pattern in model neocortical neurons. Nature. 1996; 382:363–366. [PubMed: 8684467]

Matsumoto H, Ayala GF, Gumnit RJ. Effects of intracellularly injected currents on the PDS and the hyperpolarizing after-potential in neurons within an epileptic focus. Electroencephalogr Clin Neurophysiol. 1969; 26:120. [PubMed: 4183218]

McCormick DA. Neurotransmitter actions in the thalamus and cerebral cortex and their role in neuromodulation of thalamocortical activity. Prog Neurobiol. 1992; 39:337–388. [PubMed: 1354387]

McCormick DA, Prince DA. Noradrenergic modulation of firing pattern in guinea pig and cat thalamic neurons, in vitro. J Neurophysiol. 1988; 59:978–996. [PubMed: 3367206]

Meeren HK, Pijn JP, Van Luijtelaar EL, Coenen AM, Lopes da Silva FH. Cortical focus drives widespread corticothalamic networks during spontaneous absence seizures in rats. J Neurosci. 2002; 22:1480–1495. [PubMed: 11850474]

Midzyanovskaya IS, Salonin DV, Bosnyakova DY, Kuznetsova GD, van Luijtelaar EL. The multiple effects of ketamine on electroencephalographic activity and behavior in WAG/Rij rats. Pharmacol Biochem Behav. 2004; 79:83–91. [PubMed: 15388287]

Neckelmann D, Amzica F, Steriade M. Spike-wave complexes and fast components of cortically generated seizures. III. Synchronizing mechanisms. J Neurophysiol. 1998; 80:1480–1494. [PubMed: 9744953]

Neckelmann D, Amzica F, Steriade M. Changes in neuronal conductance during different components of cortically generated spike-wave seizures. Neuroscience. 2000; 96:475–485. [PubMed: 10717428]

Nicholas AP, Pieribone V, Hokfelt T. Distributions of mRNAs for alpha-2 adrenergic receptor subtypes in rat brain: an in situ hybridization study. J Comp Neurol. 1993; 328:575–594. [PubMed: 8381444]

Niedermeyer, E. Abnormal EEG patterns: epileptic and paroxysmal. In: Niedermeyer, E.; Lopes de Silva, F., editors. Electroencephalography: Basic Principles, Clinical Applications, and Related Fields. Baltimor MD: Williams & Wilkins; 2005a. p. 255-280.

Niedermeyer, E. Epileptic seizure disorders. In: Niedermeyer, E.; Lopes de Silva, F., editors. Electroencephalography: Basic Principles, Clinical Applications, and Related Fields. Baltimor MD: Williams & Wilkins; 2005b. p. 505-620.

Nita D, Cissé Y, Timofeev I, Steriade M. Increased propensity to seizures after chronic cortical deafferentation in vivo. J Neurophysiol. 2006; 95:902–913. [PubMed: 16236784]

Nita DA, Cisse Y, Timofeev I. EPSP depression following neocortical seizures in cat. Epilepsia. 2008; 49:705–709. [PubMed: 18031546]

Nita DA, Cisse Y, Timofeev I, Steriade M. Waking-sleep modulation of paroxysmal activities induced by partial cortical deafferentation. Cereb Cortex. 2007; 17:272–283. [PubMed: 16495431]

Nuñez A, Amzica F, Steriade M. Electrophysiology of cat association cortical cells in vitro: Intrinsic properies and synaptic responses. J Neurophysiol. 1993; 70:418–430. [PubMed: 8395586]

Ohtahara S, Ohtsuka Y, Kobayashi K. Lennox-Gastaut syndrome: a new vista. Psychiatry Clin Neurosci. 1995; 49:S179–S183. [PubMed: 8612138]

Pan E, Stringer JL. Role of potassium and calcium in the generation of cellular bursts in the dentate gyrus. J Neurophysiol. 1997; 77:2293–2299. [PubMed: 9163358]

Perez Velazquez JL, Carlen PL. Gap junctions, synchrony and seizures. Trends Neurosci. 2000; 23:68–74. [PubMed: 10652547]

Pinault D, Leresche N, Charpier S, Deniau JM, Marescaux C, Vergnes M, Crunelli V. Intracellular recordings in thalamic neurones during spontaneous spike and wave discharges in rats with absence epilepsy. J Physiol. 1998; 509:449–456. [PubMed: 9575294]

Polack P-O, Charpier S. Intracellular activity of cortical and thalamic neurons during high-voltage rhythmic spike discharge in Long-Evans rats in vivo. J Physiol. 2006; 571:461–476. [PubMed: 16410284]

Pumain R, Kurcewicz I, Louvel J. Fast extracellular calcium transients: involvement in epileptic processes. Science. 1983; 222:177–179. [PubMed: 6623068]

Rudolph U, Antkowiak B. Molecular and neuronal substrates for general anesthetics. Nat Rev Neurosci. 2004; 5:709–720. [PubMed: 15322529]

Rulkov NF, Timofeev I, Bazhenov M. Oscillations in large-scale cortical networks: map-based model. J Comput Neurosci. 2004; 17:203–223. [PubMed: 15306740]

Schmitz D, Schuchmann S, Fisahn A, Draguhn A, Buhl EH, Petrasch-Parwez E, Dermietzel R, Heinemann U, Traub RD. Axo-axonal coupling a novel mechanism for ultrafast neuronal communication. Neuron. 2001; 31:831–840. [PubMed: 11567620]

Sitnikova E, van Luijtelaar G. Reduction of adrenergic neurotransmission with clonidine aggravates spike-wave seizures and alters activity in the cortex and the thalamus in WAG/Rij rats. Brain Res Bull. 2005; 64:533–540. [PubMed: 15639550]

Somjen GG. Ion regulation in the brain: implications for pathophysiology. Neuroscientist. 2002; 8:254–267. [PubMed: 12061505]

Steriade M, Amzica F. Intracellular study of excitability in the seizure-prone neocortex in vivo. J Neurophysiol. 1999; 82:3108–3122. [PubMed: 10601445]

Steriade M, Amzica F, Neckelmann D, Timofeev I. Spike-wave complexes and fast components of cortically generated seizures. II. Extra- and intracellular patterns. J Neurophysiol. 1998a; 80:1456–1479. [PubMed: 9744952]

Steriade M, Contreras D. Relations between cortical and thalamic cellular events during transition from sleep patterns to paroxysmal activity. J Neurosci. 1995; 15:623–642. [PubMed: 7823168]

Steriade M, Contreras D. Spike-wave complexes and fast components of cortically generated seizures. I. Role of neocortex and thalamus. J Neurophysiol. 1998; 80:1439–1455. [PubMed: 9744951]

Steriade M, Timofeev I. Corticothalamic operations through prevalent inhibition of thalamocortical neurons. Thalamus & related systems. 2001; 1:225–236.

Steriade M, Timofeev I, Dürmüller N, Grenier F. Dynamic properties of corticothalamic neurons and local cortical interneurons generating fast rhythmic (30–40 Hz) spike bursts. J Neurophysiol. 1998b; 79:483–490. [PubMed: 9425218]

Taylor CP, Dudek FE. Synchronous neural afterdischarges in rat hippocampal slices without active chemical synapses. Science. 1982; 218:810–812. [PubMed: 7134978]

Taylor CP, Dudek FE. Excitation of hippocampal pyramidal cells by an electrical field effect. J Neurophysiol. 1984a; 52:126–142. [PubMed: 6086853]

Taylor CP, Dudek FE. Synchronization without active chemical synapses during hippocampal afterdischarges. J Neurophysiol. 1984b; 52:143–155. [PubMed: 6086854]

Timofeev I, Grenier F, Bazhenov M, Sejnowski TJ, Steriade M. Origin of slow cortical oscillations in deafferented cortical slabs. Cereb Cortex. 2000; 10:1185–1199. [PubMed: 11073868]

Timofeev I, Grenier F, Steriade M. Spike-wave complexes and fast components of cortically generated seizures. IV. Paroxysmal fast runs in cortical and thalamic neurons. J Neurophysiol. 1998; 80:1495–1513. [PubMed: 9744954]

Timofeev I, Grenier F, Steriade M. The role of chloride-dependent inhibition and the activity of fast-spiking neurons during cortical spike-wave seizures. Neuroscience. 2002; 114:1115–1132. [PubMed: 12379264]

Timofeev I, Steriade M. Neocortical seizures: initiation, development and cessation. Neuroscience. 2004; 123:299–336. [PubMed: 14698741]

Topolnik L, Steriade M, Timofeev I. Partial cortical deafferentation promotes development of paroxysmal activity. Cereb Cortex. 2003; 13:883–893. [PubMed: 12853375]

Traub RD, Borck C, Colling SB, Jefferys JG. On the structure of ictal events in vitro. Epilepsia. 1996; 37:879–891. [PubMed: 8814102]

Traub RD, Contreras D, Cunningham MO, Murray H, LeBeau FEN, Roopun A, Bibbig A, Wilent WB, Higley MJ, Whittington MA. Single-column thalamocortical network model exhibiting gamma oscillations, sleep spindles, and epileptogenic bursts. J Neurophysiol. 2005; 93:2194–2232. [PubMed: 15525801]

Tsodyks MV, Markram H. The neural code between neocortical pyramidal neurons depends on neurotransmitter release probability. Proc Natl Acad Sci U S A. 1997; 94:719–723. [PubMed: 9012851]

Xiang Z, Huguenard JR, Prince DA. Cholinergic switching within neocortical inhibitory networks. Science. 1998; 281:985–988. [PubMed: 9703513]

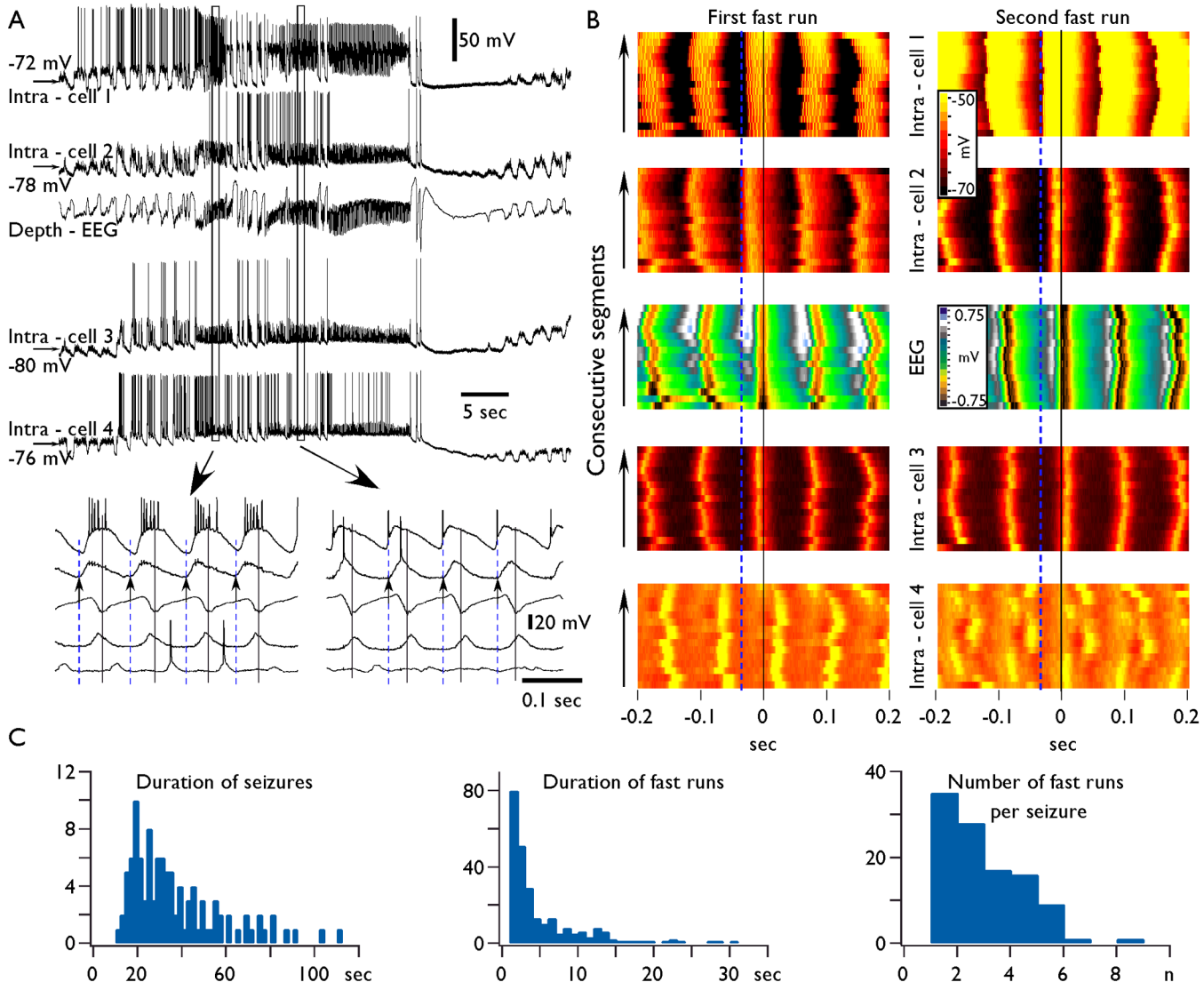

Fig. 1. Synchronization of field potential and intracellular activities during paroxysmal fast runs

A. Simultaneous depth-EEG and quadruple intracellular recordings. The electrodes were equally distributed from anterior to posterior parts of suprasylvian gyrus. The intra-cell 1 was in the anterior part of area 5 and the intra-cell 4 was in the posterior part of area 21. Encircled fragments are expanded below as indicated by arrows. Small deflections seen in expanded periods of intracellular recordings are attributed to capacitive coupling. B. Fifteen consecutive segments taken during the first and the second fast run (from panel A) for each cell are color coded for their membrane potential (see calibration bar). The segments were selected as following: the maximum of field potential depth negativity is taken as zero time and from this time point, a segment of ± 200 ms was extracted in each intracellular recording. Note that in both periods, the first maximum of depolarization in neuron 1 and 2 preceded the maximum in the field potential, the neuron 3 slightly preceded the field potential during the first shown period and followed the field during the second period, and finally the neuron 4 followed the field with constant delay during the first period and showed “patchy” pattern during the second period, during which, some cycles had similar delays, the next group of cycles was either not involved in the activity or had another delay in respect to the field. Vertical black lines indicate the maximum of depth negativity.

Vertical dashed blue lines indicate the onset of the depolarized component of fast run being electrode *Intra-cell 2* during the first fast run episode (left) and electrode *Intra-cell 1* during the second one (right). C. Summary data showing histograms of distribution of seizures duration, individual fast run duration, and the number of fast runs per seizure.

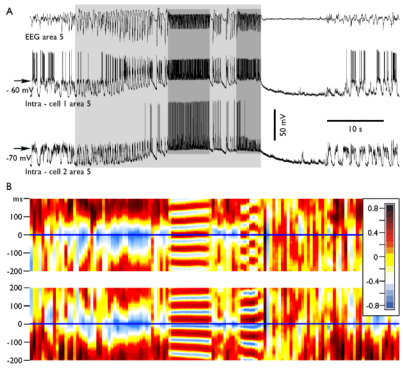

Fig. 2. Dynamics of cross-correlation during paroxysmal fast runs

A. Depth-EEG and dual intracellular recordings during a seizure containing two periods of fast runs. B, the consecutive cross-correlations between EEG and neurons. The running correlogram was calculated as following: for a time interval of 1.0 s, the correlation function between two channels was calculated with correlation length ±0.2 s. Frame was then moved with a step of 0.5 s, correlation calculated, color coded, plotted, and so on. Each of correlated periods is represented as a single color strip in the bottom panels. Note that during spike-wave discharges the correlation between neuron and EEG was negative, as expected. During the first period of fast runs, the neuron 1 had reversed phase relations with EEG, while during the second period of fast runs the neuron revealed a patchy pattern. It oscillated several cycles in phase and another several cycles in counter phase; the neuron 2 oscillated in phase with the EEG during both spike-wave complexes and during both periods of fast runs.

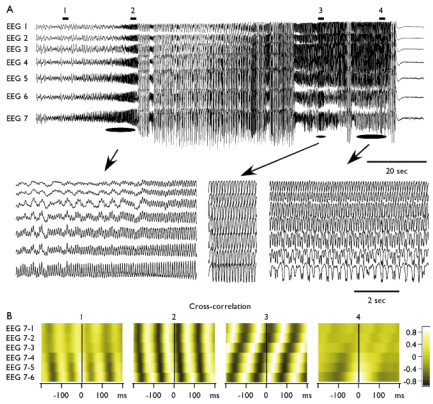

Fig. 3. Progressive involvement and variability of synchronous patterns during fast runs

A. Seven depth-EEG recordings were obtained from suprasylvian gyrus with inter-electrode distance of 1.5 mm. The seizure started with the runs of fast spikes recorded with electrode 7 (most anterior), the other electrodes reveal a progressive involvement of suprasylvian gyrus in the fast run. After several spike-wave/polyspike-wave complexes, the next period of fast runs was accompanied with perfect synchrony over suprasylvian gyrus. At the end of the seizure, the oscillatory activity with frequency around 10 Hz was found at electrode 1 and progressively declined to the electrode 7. B. Correlation analysis. Cross-correlations were obtained from periods of 2 seconds as indicated by horizontal bars and numbers in the panel A. Electrode 7 was taken as reference. At the beginning (1) and at the end (4) of seizure, the correlation between anterior and posterior electrodes was low. During periods indicated as 2 and 3 the correlation between different electrodes was high; the activity was propagating, but the propagation occurred in two different directions.

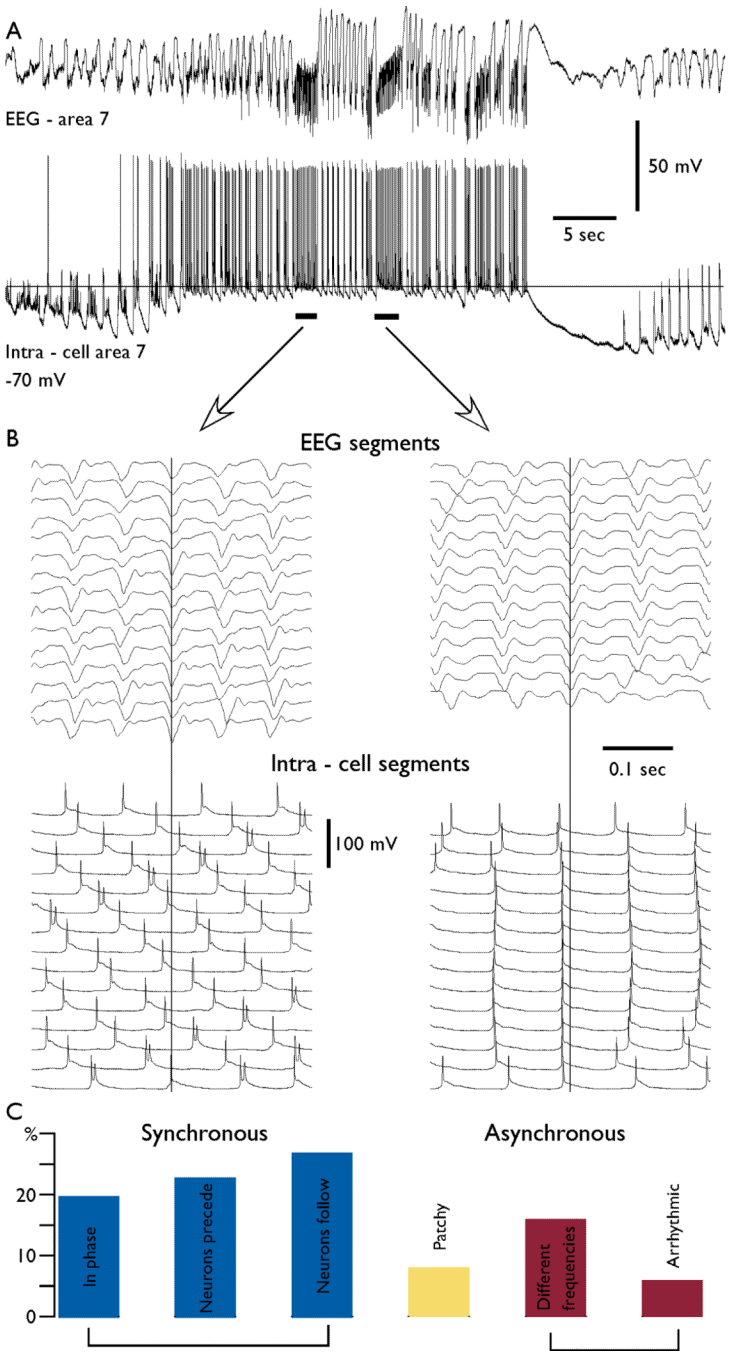

Fig. 4. Variability in neuron – field synchronization during fast runs

A. Depth-EEG and simultaneous intracellular recordings during an electrographic seizure. The distance between field potential electrode and intracellularly recorded neuron was 2 mm. B. A superposition of field potential (upper panels) and intracellular recordings (lower panels) during fast runs for the two consecutive periods of fast runs. Note the different frequencies of oscillations in the EEG and intracellularly recorded neuron during the first period and in phase synchronization during the second period. C. the distribution of patterns of synchronization for 312 periods of fast runs. The coherent patterns (0 time lag or with phase shift) constituted 70 % of cases. Arrhythmic stands for periods of fast runs recorded at one electrode, while the activity in another electrode was not rhythmic.

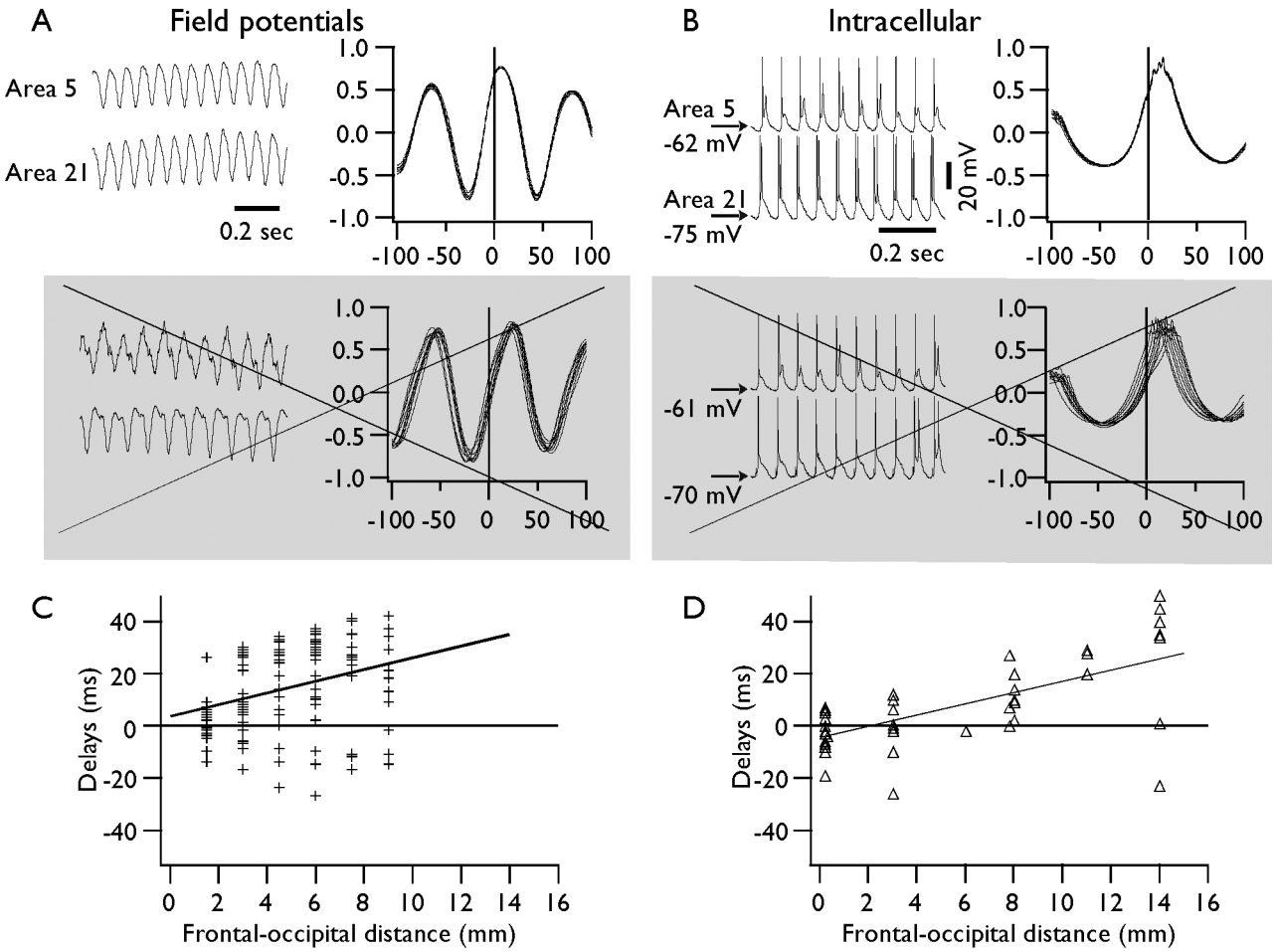

Fig. 5. Propagation of fast run activity during coherent oscillations

A. Upper left – a fragment of field potential recordings during fast runs; upper right – crosscorrelation for 10 consecutive cycles of highly coherent activity. Lower panels – examples of field potential activity and crosscorrelation in which the frequency of activity was slightly different in the two electrodes. Such periods were not included in the analysis of propagation shown in C (indicated by crossed out and grey panels). B and D. The same arrangement as in A and C, but for dual intracellular recordings.

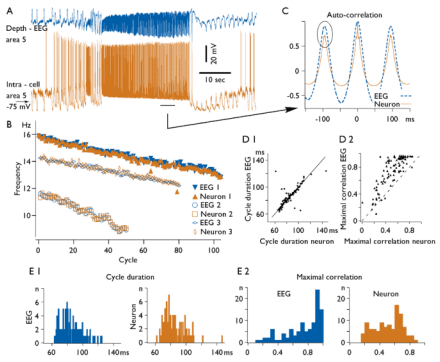

Fig. 6. Frequency of fast runs and their modulation during seizure

A. An example of electrographic seizure containing a prolonged period of fast runs. B. Instantaneous frequency of oscillation during fast runs: filled symbols for field potential and neuron shown in panel A, empty symbols - examples from two other recordings. Note a progressive decrease in the frequency of the fast run. C. Autocorrelation of EEG and intracellular activities from 5 s period indicated in the panel A. Note, lower values of maximal correlation obtained from intracellular traces as compared to EEG traces indicated by oval. D 1. The frequency relation between EEG and intracellular recordings. and D 2. Maximal autocorrelation relation between EEG and intracellular recordings. Note that in the majority of cases the frequency of fast runs at EEG and intracellular levels was similar. In the vast majority of cases the amplitude of autocorrelation for EEG traces was higher then for intracellular traces. E 1. Histograms of cycle duration for EEG (left) and intracellular recordings (right). E 2. Maximal correlation values for EEG (left) and intracellular (right) recordings.

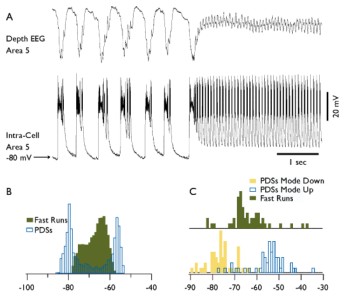

Fig. 7. Membrane potential of cortical neurons during spike-wave and fast run components of seizures

A. Field potential and intracellular recordings during a fragment of electrographic seizure containing spike-wave complexes and a fast run period. B. Histogram of membrane potential during spike-waves (transparent bars) and fast run (green bars) from the neuron shown in A. Note the presence of two peaks during spike-wave complexes and one peak during fast runs. PDS stands for paroxysmal depolarizing shift. C. Distribution of membrane potential for hyperpolarized mode of spike-wave discharges (yellow bars), for depolarized mode of spike-wave discharges (transparent bars), and for fast runs (green bars). Bins are 1 mV for histograms in B and C.

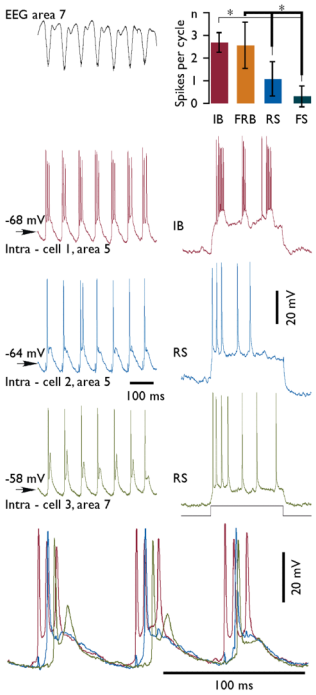

Fig. 8. Discharge patterns of variable electrophysiological types of neurons during fast runs

Left column – field potential and simultaneous triple intracellular recording during a period of fast run. Histogram at upper right corner displays a mean number of spikes generated by neurons of different electrophysiological types during each cycle of paroxysmal fast runs. Electrophysiological identification of neurons from left column is indicated at right. IB – intrinsically-bursting, FRB – fast-rhythmic-bursting, RS – regular spiking neuron, and FS – fast spiking neurons. Statistically significant difference (alpha 0.01) is indicated by asterisks. Bottom panel shows the last three cycles of cells presented in the left column at expanded scale. Note that IB cell was depolarized before the two other neurons. Note also the change of delays for depolarization of the green cell compared to the two other cells.

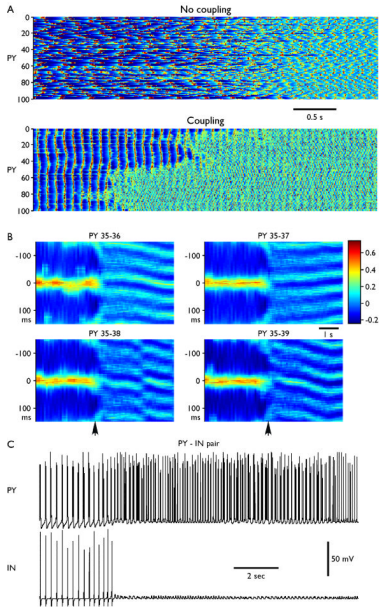

Fig. 9. Oscillations in the network model (100 PY and 25 IN neurons)

DC stimulus was presented for 10 s (from t=8 s to t=18 s) to all PY neurons and was followed by slow bursting and then by fast oscillations. (A) Network activity near the transition from slow bursting to fast runs. Top, no coupling ($g_{PY\text{-}PY}$=0, $g_{PY\text{-}IN}$=0, $g_{IN\text{-}PY}$=0), time interval from t=19 s to t=26 seconds. Bottom, coupled network ($g_{PY\text{-}PY}$=0.07 μS, $g_{PY\text{-}IN}$=0.07 μS, $g_{IN\text{-}PY}$= 0.05 μS), time interval from t=26 s to t=33 seconds. Numbers on Y axis represent the pyramidal cell number (PY #1–100). (B) Cross-correlations (sliding window, 500 ms duration, 100 ms time steps) between one PY neuron (PY35) and its neighbors (PY36-PY39). Vertical arrows indicate transition from slow bursting to fast runs. Oscillations were highly synchronized with zero phase shift in the bursting mode. During fast run, oscillations in the neighbor PY cells displayed variable phase shift (local activity propagation) with sudden phase changes. (C) Reciprocally connected PY-IN pair. Change of the $[K^+]_o$ induced transition from slow (2–3 Hz) to fast (10–15 Hz) oscillations. Bursts of spikes (but not tonic spiking) in PY neuron induced spikes in the inhibitory interneuron.